Absorbing boundary in one-dimensional anomalous transport

G. Zumofen[1] and J. Klafter[2]
[1]Laboratorium für Physikalische Chemie, Eidgenössische Technische Hochschule Zentrum, CH-8092 Zürich, Switzerland
[2]School of Chemistry, Tel-Aviv University, Tel-Aviv, 69978 Israel
(Received 7 November 1994)

In this paper we study the space-time probability distribution $Q(x,t)$ of a random walk subject to the absorbing boundary at the origin $x=0$ for motion controlled by Lévy flights and Lévy walks characterized by the exponent γ. We find that the method of images, usually applicable to Brownian motion, may break down for Lévy processes. We calculate the distribution $Q(x,t)$ to be at $x>0$ after time $t>0$ having started at the origin assuming that the boundary is effective at time $t>0$. We show that $Q(x,t)$ depends on the details of the underlying process, $Q(x,t)\sim x^{\gamma/2}/t^{1+1/\gamma}$, $1\leq\gamma\leq 2$ for small x, while total survival is independent of the spatial realization of motion and displays a universal behavior. We also discuss the related Smoluchowski boundary condition problem.

PACS number(s): 05.40.+j, 47.52.+j, 82.20.−w, 02.50.−r

I. INTRODUCTION

A large number of dynamical problems can be formulated as transport problems in half space with an absorbing boundary. Examples are found in radiation transfer [1,2], recombination of particles [3,4], heat conduction [5], filtering methods [6,7], transport along fibers, and related trapping problems [8]. While the interest has been mainly in transport in half space via Brownian motion, extensions to non-Brownian behavior have also been proposed [2,4,9].

In this paper we investigate the statistical properties of transport in one dimension with an absorbing boundary at the origin and with emphasis on motion by Lévy flights and walks. Lévy flights and walks have been discussed in detail quite extensively [10]; they give rise to enhanced diffusion as observed in dynamical systems, both dissipative and conservative [11,12]. In particular we study $Q(x,t)$, the probability density to be at $x>0$ after time $t>0$ having started at the origin. In order to avoid ambiguity in the definition of the initial conditions we assume that the absorbing boundary is effective for time $t>0$. This assumption is the continuous-time and continuous-space counterpart of the definition for the lattice model with fixed time steps introduced in Appendix A. An equivalent definition can be given by assuming that the particle starts close to the origin and that the boundary is effective at all times. The asymptotic behavior, however, is expected to be independent of this difference in the initial conditions. $Q(x,t)$ is basically the density profile due to absorbing boundary conditions and gives the functional dependence of the depletion zone near the boundary. We reestablish the relationship between $Q(x,t)$ in the presence of the absorbing boundary and the free propagator $P(x,t)$; their logarithms are related by the Hilbert transformation. We study the asymptotic forms of $Q(x,t)$ analytically and numerically and show that the characteristics of the Lévy process are reflected in the probability distribution $Q(x,t)$, while the integrated survival probability is independent of the nature of the transport. This concurs with recent findings by Frisch and Frisch [2].

The paper is organized as follows. In Sec. II we briefly review the idea of Lévy flights and Lévy walks. In Sec. III we introduce the relationship between the density profile $Q(x,t)$ and the propagator $P(x,t)$ and analyze the typical behaviors obtained for Brownian and non-Brownian (Lévy type) motion. The method of images is shown not to hold in general. We end with discussions of the related Lévy-controlled Smoluchowski boundary problem.

II. LÉVY FLIGHTS AND WALKS

In this section we discuss Lévy flights and Lévy walks for which the typical displacements grow faster than those in Brownian motion. Lévy flights have been introduced in the search for distributions for which the shape of the spatial probability distribution, the propagator, is independent of the number of steps performed in time t [10]. This requirement is naturally fulfilled by Gaussian distributions of the single step displacement. The generalization of the Gaussian case leads to the Lévy stable distributions $L_\gamma(x)$. For $\gamma=1$ we recover the Cauchy distribution and for $\gamma=2$ the Gaussian distribution. For $\gamma<2$ the large-scale behavior is characterized by a power law $L_\gamma(x)\sim|x|^{-\gamma-1}$ and consequently the variance diverges, or more generally $\langle|x|^\mu\rangle=\infty$ for $\mu\geq\gamma$. As mentioned the typical length grows faster than that in Brownian motion, namely, $\langle|x|\rangle\sim t^{1/\gamma}$ for $1<\gamma\leq 2$. This property has made the Lévy flights natural candidates for the description of enhanced diffusion [10–13].

In diffusion problems the mean-squared displacement $\langle|x|^2\rangle$ is usually considered as the central quantity in the calculations of transport properties. Here a difficulty arises due to the fact that for the Lévy stable laws the variance of a single step diverges and thus also the mean-squared displacement diverges at any time instance. This puts a limitation on the applicability of Lévy flights to physical systems. Ways to avoid this difficulty are to in-

 ©1995 The American Physical Society

troduce cutoffs in the distribution [14] or to disregard higher moments $\mu \geq \gamma$ for the description of the motion. A powerful method has recently been proposed based on a more realistic physical picture, namely, to take into account the fact that the velocity of the particle under consideration is finite. Thus the particle's motion is restricted by its velocity. Assuming a constant velocity, one has $|x| \leq vt$. This has led to the introduction of a time cost into the single event probability distributions [10–13]

$$\psi(x,t)=\delta(|x|-vt)L_{\gamma}(x) , \tag{1}$$

where $\psi(x,t)$ denotes the probability density of moving a distance x in time t in a single step. Equation (1) is associated with a partial relaxation of the property that the shape of the spatial distribution is independent of time t. Nevertheless, Eq. (1) has shown to be useful in providing a statistical description of transport in dissipative systems such as iterated nonlinear maps [11] and of motion in Hamiltonian systems [12]. Applications to intermittent chaotic motion, turbulent diffusion, and stochastic webs have also been considered [15].

Another aspect associated with Eq. (1) is the non-Markovian property of the walk [16]. While Lévy flights are typically Markovian, i.e., at each time instance the next step is independent of the past, for Lévy walks this property does not hold. In fact, if the walker moves in a particular direction there is some persistency so that the particle continues to move in the same direction in the next time instance. In our previous analyses we demonstrated that the spatial probability distribution for Lévy walks retains largely the properties of the flights. Differences appear for $\gamma > 1$ at the outermost wings where peaks appear which result from the fact that for distances $|x| > vt$ the propagator is terminated. The differences are more substantial for $\gamma < 1$. According to the velocity model the shapes of the probability distributions for the non-Markovian motion differ qualitatively from that of the Markovian Lévy motion [11]. In what follows we concentrate on Lévy flights which allow for an analytical treatment. We later compare the results with Lévy walk simulations.

III. ABSORBING BOUNDARY

We extend our previous considerations of Lévy flights and walks to the half space problem with an absorbing boundary at the origin. This problem arises naturally for chemical reactions controlled by enhanced diffusion. In the case of Brownian motion with an absorbing boundary one usually applies the method of images [4], namely, a walker which starts at x_0 on the right interferes with a walker starting at $-x_0$. This situation is related to that of Brownian geminate recombination where $2x_0$ corresponds to the interparticle distance at the initial time. In the method of images one writes, for the probability distributions $Q(x,t|x_0)$ to be at x, having started at x_0 at time $t=0$ and having survived until time t [4],

$$Q(x,t|x_0)=P(x-x_0,t)-P(-x-x_0,t) , \tag{2}$$

where $P(x,t)$ is the unrestricted free propagator denoting the probability density of being at x at time t having started at the origin at $t=0$. For Lévy flights in which we are interested, the propagator in Fourier space is [4,10]

$$P(k,t)=\exp(-at|k|^{\gamma}) . \tag{3}$$

Here and in what follows we consider the notation that the arguments denote the space in which the function is defined: for spatial aspects we use Fourier transforms with variable changes $x \leftrightarrow k$, for temporal aspects the Laplace transforms with variable changes $t \leftrightarrow u$, and when applying the generating function approach [4] we will use the variable interchange $n \leftrightarrow z$, where n is the number of jumps. Inserting Eq. (3) into Eq. (2) gives

$$Q(x,t|x_0)=\frac{1}{i\pi}\int_{-\infty}^{\infty}\sin(kx)\exp[-at|k|^{\gamma}+ikx_0]dk . \tag{4}$$

We concentrate on the particular case where the particle starts close to the origin. In order to derive an expression that is independent of x_0 and consistent with the expressions obtained for discrete lattices we consider the limiting form

$$\begin{aligned} Q(x,t)&=\lim_{x_0\to 0}\frac{1}{x_0}Q(x,t|x_0) \\ &=\frac{1}{\pi}\int_{-\infty}^{\infty}\sin(kx)k\exp[-at|k|^{\gamma}]dk \\ &=-2\partial_x P(x,t) . \end{aligned} \tag{5}$$

From this equation we calculate the integrated survival probability $\Phi(t)$ as

$$\begin{aligned} \Phi(t)=\int_0^{\infty}Q(x,t)dx&=-2\int_0^{\infty}\partial_x P(x,t)dx \\ &=2P(x,t)|_{x=0}\sim t^{-1/\gamma} . \end{aligned} \tag{6}$$

This result, however, is not correct for $\gamma < 2$, as we will see later, the reason being that the method of images breaks down for Lévy processes. More specifically, the method of images is applicable for motion for which the boundary is also a turning point of the trajectory. This is naturally the case for nearest-neighbor random walks or for the Wiener process. In the case of hopping motion the method still applies when the above condition is fulfilled asymptotically; this takes place for walks with finite mean-squared stepping lengths.

Instead of the method of images we follow Feller's derivation [17] in order to obtain an expression for $Q(x,t)$ (for details see Appendix A). Similar derivations can be based on the Wiener-Hopf decomposition and the Wiener-Hopf integral equations [1,17]. We adopt Eq. (A14) from Appendix A for the generating function representation in Fourier space

$$\ln Q(k,z)=\frac{i}{2\pi}\int_{-\infty}^{\infty}\frac{1}{k-q}\ln P(q,z)dq . \tag{7}$$

This equation states that the logarithm of the probability distribution $Q(k,z)$ is related to the logarithm of the free propagator $P(k,z)$ via the Hilbert transform. We consider the Cauchy principle for improper integrals and find

$$\ln Q(k,z)\simeq\tfrac{1}{2}\ln P(k,z)+\frac{i}{2\pi}\mathrm{P}\int_{-\infty}^{\infty}\frac{1}{k-q}\ln P(q,z)dq\ , \tag{8}$$

where P denotes the principal value. Upon exponentiation we arrive at

$$Q(k,z)\simeq\sqrt{P(k,z)}e^{i\phi(k,z)}\ , \tag{9}$$

where the phase $\phi(k,z)$ reads

$$\phi(k,z)=\frac{1}{2\pi}\mathrm{P}\int_{-\infty}^{\infty}\frac{1}{k-q}\ln P(q,z)dq$$

$$=-\frac{1}{2\pi}\mathrm{P}\int_{-\infty}^{\infty}\frac{1}{k-q}\ln[1-z\lambda(q)]dq\ . \tag{10}$$

Here $\lambda(k)$ denotes the structure factor and use is made of the generating function representation of the free propagator $P(k,z)=[1-z\lambda(k)]^{-1}$. For $k=0$ the phase term disappears, $\phi(k,z)|_{k=0}=0$, due to the inversion symmetry of $\lambda(k)$. Thus the survival probability can be written as

$$\Phi(z)=\int_{-\infty}^{\infty}Q(x,z)dx=Q(k,z)|_{k=0}\simeq\frac{1}{\sqrt{1-z}}\ . \tag{11}$$

This result is central to our study and has been discussed by Frisch and Frisch [2]. It demonstrates that $\Phi(z)$ is insensitive to the structure factor $\lambda(k)$. This contrasts with the γ-dependent result of Eq. (6), which is based on the method of images. In order to obtain an explicit time dependence we introduce the continuous-time formalism. Here

$$\mathcal{L}_{t\to u}\{Q(k,t)\}=Q(k,u)=\Psi(u)Q[k,z=\psi(u)]\ , \tag{12}$$

where $\psi(t)$ is the waiting time distribution of the single jump and $\Psi(t)$ is the probability of not having jumped until time t [18]

$$\Psi(t)=\int_{t}^{\infty}\psi(t')dt'\ . \tag{13}$$

We assume an exponential behavior for the temporal part so that $\psi(t)=\tau^{-1}e^{-t/\tau}$. For the structure factor we take the Lévy stable law

$$\lambda(k)=\exp(-b|k|^{\gamma}),\quad 1\le\gamma\le 2\ . \tag{14}$$

For simplicity we define length and time in terms of dimensionless units and set $b=\tau=1$; in the final expressions for the coefficients we will reintroduce b and τ. We concentrate on the asymptotic long-time behavior, i.e., on small-u and -k values. Using Eq. (9) we arrive at the following absolute value:

$$|Q(k,u)|\simeq\frac{1}{\sqrt{u+|k|^{\gamma}}}\ . \tag{15}$$

The derivation of asymptotic forms of the phase $\phi(k,u)$ is presented in Appendix B. For the characteristic behavior of $Q(x,t)$ we study the two asymptotic regimes $x\to 0$ and ∞. In the former case, large-k values have to be considered for which we use the approximate forms according to Eqs. (B11), (B14), and (B16)

$$\phi(k,u)\simeq\begin{cases}c_2+\dfrac{u\ln u}{\pi k}, & \gamma=1\\ c_2-c_1\dfrac{u^{1/\gamma}}{k}, & 1<\gamma<2\\ \arctan\left[\dfrac{k}{\sqrt{u}}\right], & \gamma=2.\end{cases} \tag{16}$$

Because of the symmetry relations in Eqs. (A15) and (A16), we are free to apply the Fourier sine or Fourier cosine back transforms. For the small-x regime we choose for convenience the sine transform and take the imaginary part of $Q(k,u)$

$$\mathrm{Im}Q(k,u)\sim\frac{1}{\sqrt{u+|k|^{\gamma}}}\sin\left[c_2-c_1\frac{u^{1/\gamma}}{k}\right]\ . \tag{17}$$

To first order in $u^{1/\gamma}/k$ we have

$$\mathrm{Im}Q(k,u)\sim\frac{1}{|k|^{\gamma/2}}\left[\mathrm{sinc}_2-\mathrm{cosc}_2\frac{c_1u^{1/\gamma}}{k}\right], \tag{18}$$

which upon Laplace inversion ($u\to t$) yields

$$Q(k,t)\sim\frac{-c_1\,\mathrm{cosc}_2}{\Gamma(-1/\gamma)}\frac{1}{|k|^{\gamma/2}}\frac{1}{k}t^{-1-1/\gamma},\quad 1\le\gamma<2\ . \tag{19}$$

Fourier sine inversion ($k\to x$) leads to the expression

$$Q(x,t)\sim c_3x^{\gamma/2}/t^{1+1/\gamma}=c_3\xi^{\gamma/2}/t^{1/2+1/\gamma}\ ,$$

$$\xi\to 0\ , \tag{20}$$

where ξ is the scaling variable $\xi=x/t^{1/\gamma}$. The constant c_3 is

$$c_3=\frac{\Gamma(1+1/\gamma)}{\pi\Gamma(1+\gamma/2)}\frac{\tau^{1+1/\gamma}}{b^{3/2}}\ , \tag{21}$$

where we reintroduced the constants b and τ. For the Cauchy $\gamma=1$ case we find similarly

$$\mathrm{Im}Q(k,u)\sim\frac{1}{\sqrt{|k|}}\left[\sin\frac{\pi}{4}+\cos\frac{\pi}{4}\frac{u\ln u}{\pi k}\right]\ . \tag{22}$$

Laplace inversion ($u\to t$) leads to

$$Q(k,t)\sim\frac{\cos(\pi/4)}{\pi}\frac{1}{\sqrt{|k|}}\frac{1}{kt^2},\quad \gamma=1\ , \tag{23}$$

which is Eq. (19) for $\gamma=1$; thus Eq. (19) holds also for this γ value. For the Gaussian case of $\gamma=2$ we consider the arctan representation of $\phi(k,u)$ so that

$$Q(k,u)\simeq\frac{1}{\sqrt{u+k^2}}\exp\left[i\arctan\frac{k}{\sqrt{u}}\right]$$

$$=\frac{1}{\sqrt{u}+ik},\quad \gamma=2\ , \tag{24}$$

which upon Fourier and Laplace inversion leads to Eq. (5), i.e., a result that coincides with that of the method of images and shows the short-range behavior which is consistent with Eq. (20).

We notice that $Q(x,t)$ of Eq. (20) increases as a power

law in the scaling variable ξ with the exponent $\gamma/2$, which corresponds to the linear behavior of the Gaussian $\gamma=2$ case. The power-law prefactor in t is that of the regular propagator corrected by $t^{-1/2}$, which is due to the overall decay, as we show below.

We now analyze the large-x behavior. Here the small-k regime in Eqs. (B8) is relevant, which favors the application of the Fourier cosine back transformation. We approximate the cosine part of the phase by

$$\cos\phi(k,u)\simeq 1, \quad k \ll u^{1/\gamma} , \tag{25}$$

so that the real part of $Q(k,u)$ is

$$\mathrm{Re}Q(k,u)\sim \frac{1}{\sqrt{u+|k|^{\gamma}}}, \quad |k| \ll u^{1/\gamma} , \tag{26}$$

which upon Laplace inversion ($u\rightarrow t$) yields

$$\mathrm{Re}Q(k,t)\sim \frac{1}{\sqrt{\pi t}}\exp(-t|k|^{\gamma}), \quad t|k|^{\gamma}\ll 1 . \tag{27}$$

We notice that up to the $(\pi t)^{-1/2}$ prefactor, we have recovered the stable law. Thus for large ξ

$$Q(x,t)\sim c_4\xi^{-\gamma-1}t^{-1/2-1/\gamma}, \quad \xi\gg 1, \ 1\le\gamma<2 , \tag{28}$$

with

$$c_4=\frac{2}{\pi^{3/2}}\Gamma(1+\gamma)\sin(\pi\gamma/2)b^{1/\gamma}/\sqrt{\tau} . \tag{29}$$

Equation (28) shows the proper scaling behavior and a temporal power-law prefactor equal to that of the short-range behavior in Eq. (20). For $\gamma=2$ we recall that Eq. (5) has to be considered showing a tail dominated by the Gaussian.

Finally, we also give the integrated survival probability for time t. Using the fact that the phase $\phi(k,u)$ is zero for $k\rightarrow 0$, one has from Eq. (15)

$$\Phi(t)=\mathcal{L}^{-1}\{Q(k,u)|_{k=0}\}\simeq\left[\frac{\tau}{\pi t}\right]^{1/2} . \tag{30}$$

This result is equivalent to Eq. (11) and for the Gaussian $\gamma=2$ case it is consistent with Eq. (6).

We now present some numerical results. We calculated $Q(x,t)$ by a repeated convolution procedure for a discretized lattice model. A lattice of typically 2^{16}–2^{18} sites was used and the structure factor of Eq. (14) was applied. The absorbing boundary was realized according to Eq. (A2), i.e., $Q_0(j=0)=1$ and $Q_0(j)=0, j>0$, as the initial conditions and $Q_n(j)=0$, $j\le 0$, for steps $n>0$. The repeated convolution according to Eq. (A3) was calculated by a fast Fourier transform.

In Fig. 1 we show the numerical results of the survival probability $\Phi(t)$ obtained from the integrated numerical $Q(x,t)$. The small deviations from the predictions of Eq. (30) are assigned to finite-size effects. The plotted curves demonstrate convincingly the independence of the survival probability of the exponent γ. We again stress that this result contrasts with that of Eq. (6) based on the method of images.

In Fig. 2 we show the results of $Q(x,t)$ for various γ and t values in the scaling representation. The convergence of the data towards a master curve indicates that scaling holds. The simulation results are compared with the small-ξ and large-ξ asymptotic behaviors of Eqs. (20) and (28). Good agreement with the predicted slopes and prefactors is observed in all cases.

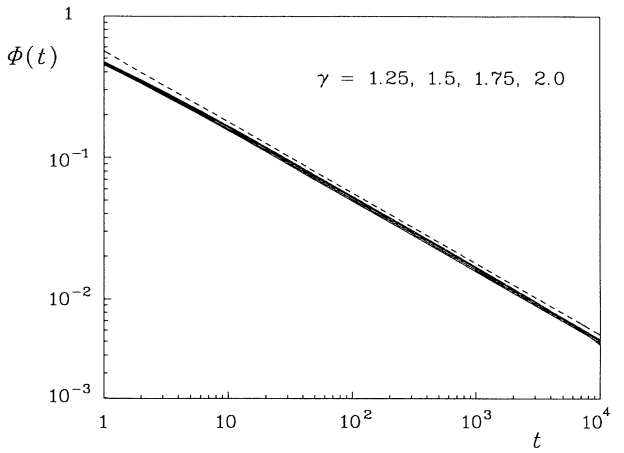

FIG. 1. Survival probability $\Phi(t)$ for Lévy flights. The simulation results are displayed as full lines for γ values equal to 1.25, 1.5, 1.75, and 2. The dashed line gives $(\pi t)^{-1/2}$ of Eq. (30). The independence of $\Phi(t)$ on γ is obvious.

To better visualize the power-law $\xi^{\gamma/2}$ behavior in the small-ξ regime and the stable-law behavior at large ξ, we give in Fig. 3 $Q(x,t)$ on linear scales. The simulation results indicate that the convergence towards the scaling behavior is slow for small ξ. The predicted power law of Eq. (20) for small ξ the numerical Fourier inversion of Eq. (27) for large ξ are shown; good agreement is observed in both cases.

Figures 4 and 5 are devoted to variants of the model.

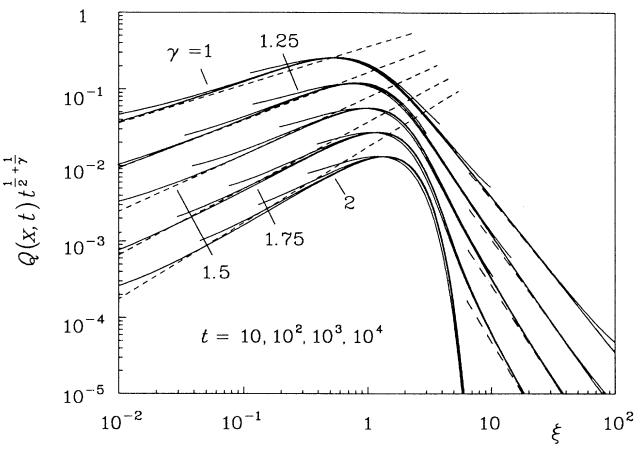

FIG. 2. Probability distribution $Q(x,t)$ of the half space problem for Lévy flights. The simulation results are given in the scaling representation as full lines for various γ values and for various times as indicated. The dashed lines give the small-ξ approximate forms of Eq. (20) and the dash-dotted lines give the large-ξ behavior of Eq. (28) for $\gamma<2$. For clarity the curves are shifted vertically with increasing γ values by factors of $\frac{1}{2}$.

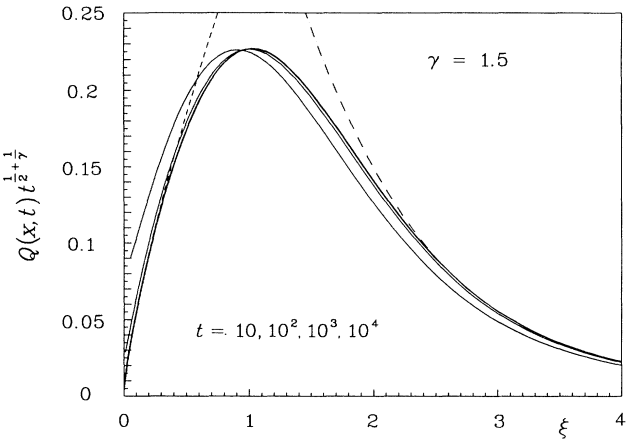

FIG. 3. Probability distribution $Q(x,t)$ for Lévy flights on linear scales for the particular case of $\gamma=1.5$. The dashed line gives the power-law form of Eq. (20) and the dash-dotted line is the result of the numerical Fourier inversion of Eq. (27).

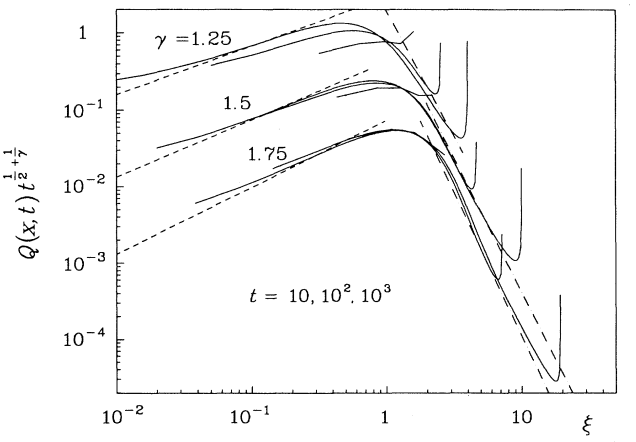

FIG. 5. Same as Fig. 4, but for Lévy walks. For clarity the curves are shifted vertically with increasing γ values by factors of $\frac{1}{3}$.

In Fig. 4 the probability profile $Q(x,t)$ is presented for a pure power-law single step distribution $\lambda(x)\sim|x|^{-\gamma-1}$, $x\neq0$. Deviations from the Lévy flight results in Fig. 2 appear for the marginal case $\gamma=2$, where the convergence to the asymptotic behavior is poor because of logarithmic corrections. For $\gamma=3$ the Gaussian case is recovered reasonably. In Fig. 5 results are presented for Lévy walks with the stepping probability $\psi(x,t)\sim\delta(|x|-t)\lambda(x)$, according to Eq. (1), and with $\lambda(x)\sim|x|^{-\gamma-1}$, $x\neq0$. An exact enumeration technique was applied, which imposes limitations on the maximum number of steps $t\leq10^3$. The computed curves behave as those of the corresponding flights in Fig. 4, but with a slower convergence for small ξ and with characteristic peaks at $|x|=t$ [11,12].

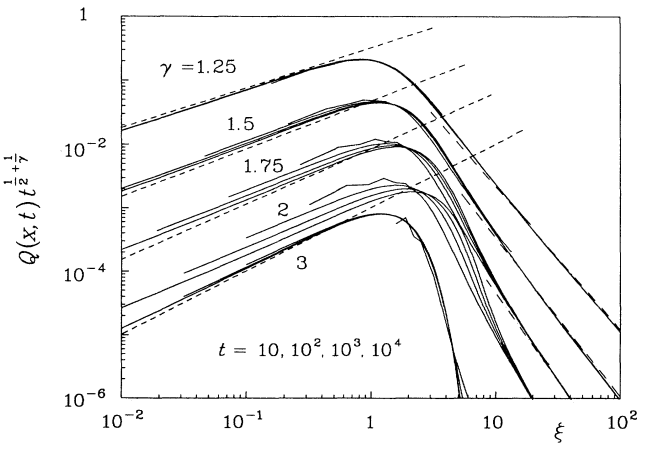

FIG. 4. Same as Fig. 2, but for $\lambda(x)\sim|x|^{-\gamma-1}$. No scaling is observed for $\gamma=2$; accordingly the theoretical slope is not displayed for this γ value. For clarity the curves are shifted vertically with increasing γ values by factors of $\frac{1}{4}$.

IV. DISCUSSION

We regard Eqs. (20) and (28), for $Q(x,t)$ in the short-ξ and the large-ξ regimes, respectively, and Eq. (30) for the survival $\Phi(t)$ as the main results of this paper. While the decay of the survival probability $\Phi(t)$ is the same for Brownian and non-Brownian (Lévy) motions, there are pronounced differences in the spatial shape of $Q(x,t)$. For small x there is a $\gamma/2$ power-law behavior which corresponds to the linear behavior in the Brownian $\gamma=2$ case. For large ξ the behavior is dominated by a Gaussian tail for Brownian motion; for Lévy flights with $\gamma\neq2$ one recovers the behavior of the corresponding free propagator. We conjecture that the γ dependence of $Q(x,t)$ extends to the regime of $\gamma<1$, i.e., the $\gamma/2$ rule for the small ξ and the stable law for large ξ hold also for $\gamma<1$. Furthermore, we conjecture that the survival $\Phi(t)$ is independent of γ also in this regime. However, we expect that there are qualitative differences between the Lévy flights and the Lévy walks in this regime.

The pronounced deviation of $Q(x,t)$ from a linear behavior for small-x values is expected to affect also the reaction dynamics controlled by enhanced diffusion [19,20]. There particle-particle correlation functions should follow the $\gamma/2$ power law for small interparticle distances. The time-dependent rates and interparticle correlation functions are often discussed in terms of the Smoluchowski boundary problem, which is the diffusion problem subject to an absorbing sphere at the origin and solved for the initial condition of a filled space. Here we study this situation for the Lévy process in one dimension using scaling arguments. We first consider $Q(x,t|x_0)$ and assume that the small-ξ behavior of Eq. (20) dominates also for $x_0\neq0$ so that

$$Q(x,t|x_0)\sim\xi^{\gamma/2}/t^{1/2+1/\gamma},\quad t\gg x_0^{\gamma},\ \xi\ll1\ , \tag{31}$$

where the limits on x_0 and ξ state that the expression holds for times for which the typical displacement is much larger than both x_0 and x. We now consider the

profile $W(x,t)$ for the initially half filled space of the Smoluchowski boundary problem and write

$$W(x,t)=\int_0^\infty Q(x,t|x_0)dx_0 \simeq \int_0^\rho Q(x,t|x_0)dx_0 \sim \xi^{\gamma/2} ,$$
$$\xi \ll 1,\ \rho \sim t^{1/\gamma} . \quad (32)$$

The upper integration limit ρ accounts for the assumption that $W(x,t)$ is dominated for small x by the surviving particles initiated close to the origin if compared with the typical displacement after time t. The behavior in Eq. (32) is compared with numerical results in Fig. 6. For the computations the procedure developed for $Q(x,t)$ was modified to account for a filled lattice at initial time $W(x,t=0)=1$, $x \geq 0$. The results show a convergence with increasing time to the asymptotic behavior, which is dominated by the $\gamma/2$ power law of Eq. (32). This indicates convincingly that the $\gamma/2$ power law really extends beyond the case of a single particle located initially in the vicinity of the origin.

In the Smoluchowski method of calculating reaction rates the flux into the origin is considered and consequently the rates are related to the gradient of the profiles at the boundary. We calculate the flux from an alternative approach which holds in one dimension and applies also for Lévy flights

$$J_0(t)=\int_{-\infty}^0 dx \int_{0^+}^\infty dy\ W(y,t)\lambda(x-y) . \quad (33)$$

Here we consider only the absolute value of the flux. A rough estimate of $J_0(t)$ can be obtained as follows: We disregard the details in the shape of $W(x,t)$ for $x \lesssim t^{1/\gamma}$ and replace $W(x,t)$ by the step function $W(x,t)\simeq 0$ for $x < t^{1/\gamma}$ and $W(x,t)\simeq 1$ for $x \geq t^{1/\gamma}$. We also approximate $\lambda(x)$ by the power law $\lambda(x)\sim |x|^{-\gamma-1}$ and obtain

$$J_0(t)\sim \int_{-\infty}^0 dx \int_{t^{1/\gamma}}^\infty dy \frac{1}{|x-y|^{\gamma+1}}$$
$$\sim t^{1/\gamma-1} , \quad (34)$$

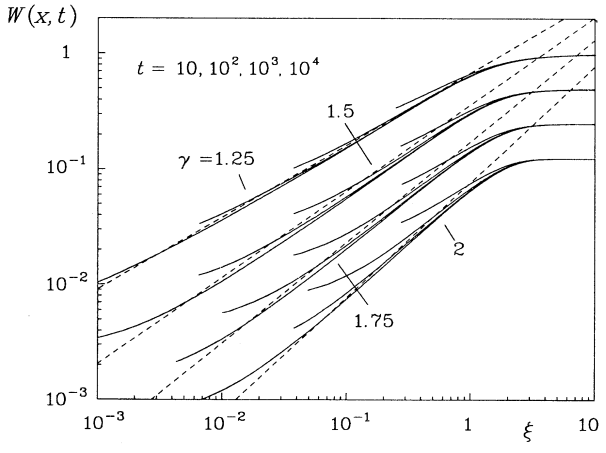

FIG. 6. Density profiles $W(x,t)$ of the Smoluchowski boundary problem for Lévy flights. Plotted is $W(x,t)$ as a function of the scaling variable $\xi=x/t^{1/\gamma}$. Full lines give the numerical results for various γ values and times as indicated. For clarity the curves are shifted vertically with increasing γ values by factors of $\frac{1}{2}$.

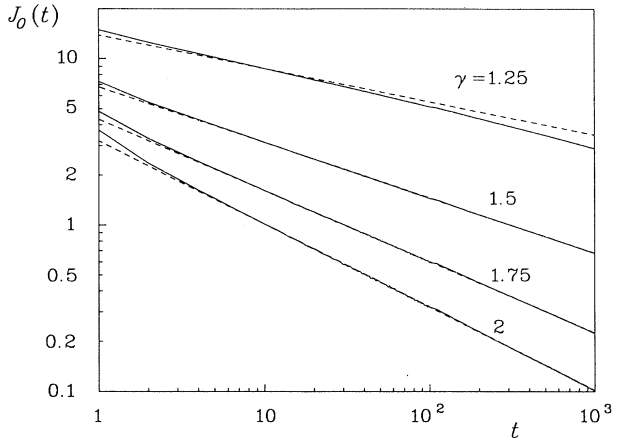

FIG. 7. Flux $J_0(t)$ of the Smoluchowski boundary problem for Lévy flights. The numerical results are plotted as full lines for various γ values as indicated. The dashed lines give the predicted behavior $t^{1/\gamma-1}$ of Eq. (34). The deviations from the prediction in the case of $\gamma=1.25$ are due to finite-size effects.

which is consistent with the time evolution of the effective volume $S(t)$ spanned by the walker $S(t)\sim t^{1/\gamma}$ [20].

In Fig. 7 we present results of the flux $J_0(t)$ as a function of time for several γ values. The plotted curves show a reasonable agreement with the predicted behavior $t^{1/\gamma-1}$. The comparison with Fig. 1 demonstrates strikingly the qualitative different behavior of $\Phi(t)$ and $J_0(t)$.

We notice that the flux $J_0(t)$ is not related to the density profile close to the origin in an obvious way. The situation is different for Brownian motion where the flux $J_0(t)$ is related to the gradient by $J_0(t) \sim -\partial_x W(x,t)|_{x=0}$. This holds for Euclidean spaces and also for fractals as was recently shown. In a speculative manner we may argue that a generalized fractional partial differential equation approach $\partial/\partial t W(x,t) = \partial^{\gamma/2}/\partial x^{\gamma/2} C \partial^{\gamma/2}/\partial x^{\gamma/2} Q(x,t)$, where C is a generalized diffusion coefficient, can be associated with a generalized gradient $\partial^{\gamma/2}/\partial x^{\gamma/2} W(x,t)$. Such a gradient seems to be consistent with the $\gamma/2$ behavior for small x; however, the linkage to the temporal behavior of the flux is lacking.

In summary, we have analyzed density profiles and survival probabilities for motion dominated by Lévy flights and Lévy walks in one-dimensional half space with an absorbing boundary. We have noticed that the method of images does not apply in general and that other techniques have to be used. We found the interesting result that the profiles behave nonlinearly at small distances and that therefore gradients in the usual sense are ill defined at the origin. In the Smoluchowski boundary condition problem the temporal behavior of the flux into the origin is consistent with previous findings of time-dependent reaction rates.

ACKNOWLEDGMENTS

We thank Professor H. Frisch and Professor U. Frisch for valuable discussions, for bringing to our attention

Feller's derivation of the half space problem, and for sending us their manuscript prior to publication. We also thank Professor K. Dressler and Shiliang Yu for interesting discussions and F. Weber for technical assistance. One of us (J.K.) thanks the ETH for support and hospitality. A grant of the Rechenzentrum ETH-Zurich is gratefully acknowledged.

APPENDIX A

In this appendix we study the relationship between the probability distribution $Q(x,t)$ for an absorbing boundary and the distribution $P(x,t)$ for the unrestricted motion. We follow Feller [17] for the derivation of an expression for $Q(x,t)$. We make use of the random-walk framework and denote the walk by x_n, the location of the walker after n jumps. x_n is the sum of n independent displacements. We define by R_n the probability of a walker to stay to the right in $n-1$ steps and to jump to the origin or to the left in the nth jump

$$R_n=\text{Prob}\{x_1>0,\ldots,x_{n-1}>0,x_n\le 0\}\ ,\qquad R_0=0\ . \tag{A1}$$

The complementary quantity is Q_n, the probability of having started at the origin and staying on the right including the nth jump

$$Q_n=\text{Prob}\{x_1>0,\ldots,x_n>0\}\ ,\qquad Q_0=\delta(x)\ . \tag{A2}$$

The following recursion holds:

$$R_{n+1}(x)+Q_{n+1}(x)=\int_{-\infty}^{\infty}Q_n(y)\lambda(x-y)dy\ , \tag{A3}$$

where $\lambda(x)$ is the unrestricted jump probability distribution for a single step. In Fourier space ($x\rightarrow k$) we have

$$R_{n+1}(k)+Q_{n+1}(k)=Q_n(k)\lambda(k)\ , \tag{A4}$$

where $\lambda(k)$ is the structure function. The generating function form is obtained from multiplication of Eq. (A4) by z^{n+1} and summation over n on both sides

$$\sum_{n=0}^{\infty}z^{n+1}[R_{n+1}(k)+Q_{n+1}(k)]=\lambda(k)\sum_{n=0}^{\infty}z^{n+1}Q_n(k)\ . \tag{A5}$$

After reorganization

$$R(k,z)+Q(k,z)-1=\lambda(k)zQ(k,z) \tag{A6}$$

and

$$1-R(k,z)=Q(k,z)[1-z\lambda(k)]\ . \tag{A7}$$

Taking the logarithms on both sides one has

$$\ln\left[\frac{1}{1-z\lambda(k)}\right]=\ln\left[\frac{1}{1-R(k,z)}\right]+\ln Q(k,z)\ , \tag{A8}$$

which upon expansion yields

$$\sum_{n=0}^{\infty}\frac{z^n}{n}[\lambda(k)]^n=\sum_{n=0}^{\infty}\frac{1}{n}[R(k,z)]^n+\sum_{n=0}^{\infty}\frac{(-1)^n}{n}[Q(k,z)-1]^n\ . \tag{A9}$$

On the left the terms are symmetric in x and range from $-\infty$ to ∞. On the right the first sum is a function defined for $x\le 0$; $Q(k,z)-1$ is defined for $x>0$ and thus also $[Q(k,z)-1]^n$ is defined for $x>0$. One may allocate to each of the terms on the right its counterpart on the left so that from (A8) we find

$$\ln Q(k,z)=\sum_{n=1}^{\infty}\frac{z^n}{n}\int_{0^+}^{\infty}e^{ikx}P_n(x)dx\ , \tag{A10}$$

where we made use of the relationship $P_n(k)=[\lambda(k)]^n$. This relation allows also for the form

$$\ln Q(k,z)=\frac{1}{2\pi}\sum_{n=1}^{\infty}\frac{z^n}{n}\int_{0^+}^{\infty}dx\,e^{ikx}\int_{-\infty}^{\infty}dq\,e^{-iqx}[\lambda(q)]^n\ . \tag{A11}$$

Integration over x yields

$$\ln Q(k,z)\simeq\frac{i}{2\pi}\sum_{n=1}^{\infty}\frac{z^n}{n}\int_{-\infty}^{\infty}\frac{1}{k-q}[\lambda(q)]^n dq\ , \tag{A12}$$

where we assumed that the equation holds approximately because the lower integration boundary in Eq. (A11) is 0^+. For discrete lattices there may be a difficulty on the scale of the lattice units and deviations may arise for short times. The summation in Eq. (A12) can be performed so that

$$\ln Q(k,z)=\frac{1}{i2\pi}\int_{-\infty}^{\infty}\frac{1}{k-q}\ln[1-z\lambda(q)]dq\ . \tag{A13}$$

Considering $[P(k,z)]^{-1}=1-z\lambda(k)$ we arrive at the central equation

$$\ln Q(k,z)\simeq\frac{i}{2\pi}\int_{-\infty}^{\infty}\frac{1}{k-q}\ln P(q,z)dq\ , \tag{A14}$$

which concurs with the Hilbert transformation. Equation (A14) is Eq. (7) of the main text; it guarantees for the symmetry relationships

$$\begin{aligned}&\mathcal{F}_s^{-1}\{\text{Im}Q(k,z)\}=\mathcal{F}_c^{-1}\{\text{Re}Q(k,z)\},\quad x>0\\&\mathcal{F}_s^{-1}\{\text{Im}Q(k,z)\}=-\mathcal{F}_c^{-1}\{\text{Re}Q(k,z)\},\quad x<0\\&\mathcal{F}_s^{-1}\{\text{Re}Q(k,z)\}=-\mathcal{F}_c^{-1}\{\text{Im}Q(k,z)\},\quad -\infty\le x\le\infty,\end{aligned} \tag{A15}$$

where $\mathcal{F}_s,\mathcal{F}_c$ denote the Fourier sine and cosine transforms and Im and Re denote the imaginary and real parts, respectively. Thus

$$Q(x,z)=2\mathcal{F}_s^{-1}\{\text{Im}Q(k,z)\}=2\mathcal{F}_c^{-1}\{\text{Re}Q(k,z)\}\ ,\qquad x>0\ . \tag{A16}$$

These expressions are used in the main text for the analysis of the asymptotic behaviors of $Q(x,t)$.

APPENDIX B

In this appendix we study the phase $\phi(k,u)$ as a function of its two arguments. Our study has been guided by the numerical investigation of $\phi(k,u)$ and we propose the following analysis of the asymptotic behavior. We first concentrate on the k dependence and distinguish between three regimes. For $k\to 0$ we make use of the lowest-order expansion in the variable q in Eq. (10). We also make use of the Saalschütz form by adding and subtracting corresponding terms in the integrand so that for $1<\gamma\leq 2$

$$\begin{aligned}\phi(k,z)&=\frac{1}{2\pi}\sum_{n=1}^{\infty}\frac{z^n}{n}\left\{\mathrm{P}\int_{-\infty}^{\infty}\frac{1}{k-q}[\exp(-n|q|^{\gamma})-1]dq\right.\\&\qquad\left.+\mathrm{P}\int_{-\infty}^{\infty}\frac{1}{k-q}dq\right\}\\&\simeq-\frac{k}{2\pi}\sum_{n=1}^{\infty}\frac{z^n}{n}\mathrm{P}\int_{-\infty}^{\infty}\frac{1}{q^2}[\exp(-n|q|^{\gamma})-1]dq\\&\simeq\frac{k}{\pi}\Gamma\left[1-\frac{1}{\gamma}\right]\sum_{n=1}^{\infty}\frac{z^n}{n^{1-1/\gamma}}\ ,\end{aligned}\tag{B1}$$

where $\Gamma(x)$ denotes the gamma function [21]. The sum converges if $z<1$. Replacing the sum by an integral and using the small-u behavior of z we arrive at

$$\phi(k,u)\simeq\csc(\pi/\gamma)k/u^{1/\gamma}\ .\tag{B2}$$

For the Cauchy $\gamma=1$ case we take advantage of the closed-form expression for the free propagator in x space, so that

$$\begin{aligned}\phi(k,u)&=\sum_{n=1}^{\infty}\frac{z^n}{n}\frac{n}{\pi}\int_{0^+}^{\infty}\frac{\sin(kx)}{n^2+k^2}dx\\&=-\frac{1}{\pi}\sum_{n=1}^{\infty}z^n\tfrac{1}{2}[e^{-nk}\mathrm{Ei}(nk)-e^{nk}E_1(nk)]\\&\simeq-\frac{k\ln k}{\pi u}\ ,\end{aligned}\tag{B3}$$

to lowest order in k and u. In Eq. (B3) $\mathrm{Ei}(x)$ and $E_1(x)$ denote the exponential integrals [21]. The logarithmic correction is consistent with the divergence of the prefactor in Eq. (B2) for $\gamma\to 1$.

Next we study the intermediate range $u^{1/\gamma}\ll k\ll 1$. We make use of the small-(k,u) approximation of $P(k,u)$ so that

$$\phi(k,u)\simeq-\frac{1}{2\pi}\mathrm{P}\int_{-\infty}^{\infty}\frac{1}{k-q}\ln(u+|q|^{\gamma})dq\ .\tag{B4}$$

To order zero in u we have

$$\begin{aligned}\phi(k,u)&\simeq-\frac{1}{2\pi}\mathrm{P}\int_{-\infty}^{\infty}\frac{1}{k-q}\ln(|q|^{\gamma})dq\\&=-\frac{\gamma k}{\pi}\int_0^{\infty}\frac{1}{k^2-q^2}\ln q\,dq\\&=\pi\gamma/4\ ,\end{aligned}\tag{B5}$$

independent of k. Finally, we consider the large $k\gg 1$ regime. We approximate the denominator $(k-q)^{-1}$ by k^{-1} and obtain

$$\begin{aligned}\phi(k,z)&\simeq\frac{1}{\pi k}\sum_{n=1}^{\infty}\frac{z^n}{n}\int_0^{\infty}\exp(-n|q|^{\gamma})dq\\&=\frac{1}{\pi k}\Gamma\left[1+\frac{1}{\gamma}\right]\sum_{n=1}^{\infty}\frac{z^n}{n^{1+1/\gamma}}\ .\end{aligned}\tag{B6}$$

The sum converges for $z=1$ so that we obtain to lowest order

$$\phi(k,u)=\frac{\Gamma(1+1/\gamma)\zeta(1+1/\gamma)}{\pi k},\quad k\gg 1\ ,\tag{B7}$$

where $\zeta(x)$ is the Riemann zeta function [21]. Summarizing the behavior of the three regimes we have

$$\phi(k,u)\simeq\begin{cases}-k\ln k/(\pi u), & k\ll u^{1/\gamma}, & \gamma=1\\ c_1k/u^{1/\gamma}, & k\ll u^{1/\gamma}, & 1<\gamma\leq 2\\ c_2, & u^{1/\gamma}\ll k\ll 1, & 1\leq\gamma\leq 2\\ c_3/k & k\gg 1, & 1\leq\gamma\leq 2,\end{cases}\tag{B8}$$

with the constants

$$\begin{aligned}c_1&=\csc(\pi/\gamma)\ ,\\c_2&=\pi\gamma/4\ ,\\c_3&=\pi^{-1}\Gamma(1+1/\gamma)\zeta(1+1/\gamma)\ .\end{aligned}\tag{B9}$$

The small-k behavior of Eq. (B8) is used in Eq. (22) of the main text. For the Gaussian $\gamma=2$ case we derive

$$\begin{aligned}\phi(k,z)&\simeq\frac{1}{2\pi}\sum_{n=1}^{\infty}\frac{z^n}{n}\mathrm{P}\int_{-\infty}^{\infty}\frac{1}{k-q}\exp(-nq^2)dq\\&=-\tfrac{1}{2}\sum_{n=1}^{\infty}z^n\sum_{j=1}^{\infty}(-1)^j\frac{k^{2j-1}n^{j-3/2}}{\Gamma(j+1/2)}\ ,\end{aligned}\tag{B10}$$

and by replacing the sum by an integral and using the small-u behavior of z we find

$$\begin{aligned}\phi(k,u)&\simeq-\tfrac{1}{2}\sum_{n=1}^{\infty}(-1)^n\frac{k^{2n-1}}{\Gamma(n+\frac{1}{2})}\int_0^{\infty}dy\,z^y y^{n-3/2}\\&\simeq-\tfrac{1}{2}\sum_{n=1}^{\infty}(-1)^n\frac{k^{2n-1}}{\Gamma(n+\frac{1}{2})}\frac{\Gamma(n-\frac{1}{2})}{u^{n+1/2}}\\&=-\sum_{n=1}^{\infty}\frac{(-1)^n}{2n-1}\left[\frac{k}{\sqrt{u}}\right]^{2n-1}\\&=\arctan\left[\frac{k}{\sqrt{u}}\right]\ .\end{aligned}\tag{B11}$$

For $(k/\sqrt{u})\to 0$ and $(k/\sqrt{u})\gg 1$ this equation is consistent with the small- and intermediate-k results of Eq. (B8).

In Fig. 8 we show the phase $\phi(k,u)$ as a function of k for various γ values. The phase was calculated numerically from Eq. (10) and is compared in the figure with the asymptotic forms of Eqs. (B8). For $\gamma=2$ the arctan representation of Eq. (B11) is considered. In all cases the numerical results corroborate the asymptotic predictions.

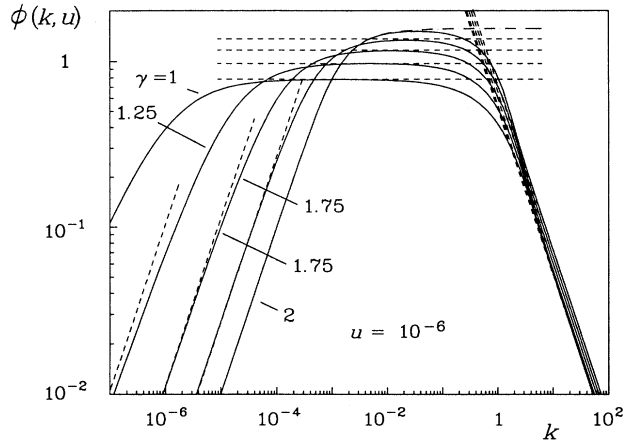

FIG. 8. k dependence of the phase $\phi(k,u)$ obtained from the numerical integration of Eq. (10). The numerical results are given by full lines as functions of k on log-log scales for $u=10^{-6}$ and for various γ values as indicated. The dashed liens show the approximate forms of Eq. (B8), except for the Cauchy $\gamma=1$ case at small k. For the Gaussian $\gamma=2$ case the dash-dotted curve is the arctan approximation of Eq. (B11).

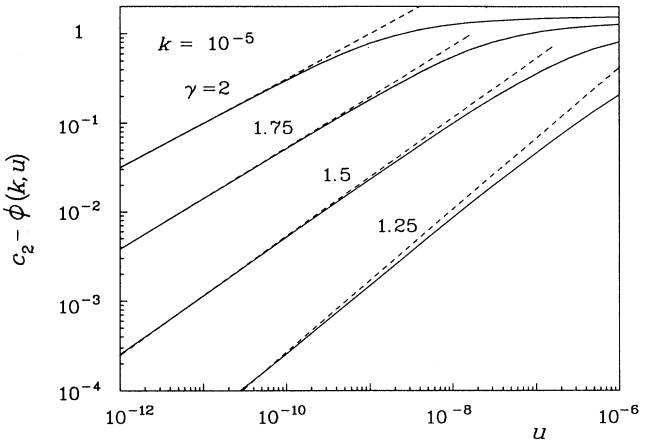

FIG. 9. u dependence of the phase $\phi(k,u)$ obtained from the numerical integration of Eq. (10). Plotted is $c_2-\phi(k,u)$ as a function of u for a fixed value of $k=10^{-5}$. The numerical results are given by full lines for various γ values as indicated. The dashed lines give $c_1 u^{1/\gamma}/k$ according to Eq. (B14).

We now concentrate on the u dependence of the phase $\phi(k,u)$. For this purpose we consider the intermediate-k regime in Eq. (B8) as a basis and subtract the constant c_2 and add the corresponding term; we obtain

$$\phi(k,z)\simeq c_2+\frac{1}{2\pi}\sum_{n=1}^{\infty}\frac{z^n-1}{n}\mathrm{P}\int_{-\infty}^{\infty}\frac{1}{k-q}\exp(-n|q|^{\gamma})dq\ . \tag{B12}$$

We again approximate the denominator $(k-q)^{-1}$ by k^{-1} and find

$$\phi(k,z)\simeq c_2+\frac{1}{2\pi k}\sum_{n=1}^{\infty}\frac{z^n-1}{n}\mathrm{P}\int_{-\infty}^{\infty}\exp(-n|q|^{\gamma})dq$$

$$\simeq c_2+\frac{1}{\pi k}\Gamma\left[1+\frac{1}{\gamma}\right]\sum_{n=1}^{\infty}\frac{z^n-1}{n^{1+1/\gamma}}\ . \tag{B13}$$

Replacing the sum by an integral and using the small-u approximation of z we recover the Saalschütz form so that

$$\phi(k,u)\simeq c_2-c_1\frac{u^{1/\gamma}}{k}\ , \tag{B14}$$

where c_1 is the constant in Eq. (B9). Analogously we obtain for the Cauchy $\gamma=1$ case

$$\phi(k,z)\simeq c_2+\frac{1}{2\pi k}\sum_{n=1}^{\infty}\frac{z^n-1}{n}\mathrm{P}\int_{-\infty}^{\infty}\exp(-n|q|)dq$$

$$\simeq c_2+\frac{1}{\pi k}\sum_{n=1}^{\infty}\frac{z^n-1}{n^2}\ . \tag{B15}$$

Replacing the sum by an integral, introducing the lower integration bound ϵ to avoid divergence, and using the small-u approximation of z we find

$$\phi(k,u)\simeq c_2+\frac{1}{\pi k}\int_{\epsilon}^{\infty}\frac{e^{-uy}-1}{y^2}dy$$

$$\simeq c_2+\frac{u\ln u}{\pi k} \tag{B16}$$

to lowest order. Again the logarithmic correction is consistent with the divergence of $c_1=\csc(\pi/\gamma)$ in Eq. (B14) for $\gamma\to 1$. The u dependence of $\phi(k,u)$ is summarized in Eq. (16) of the main text.

In Fig. 9 we show the phase $\phi(k,u)$ as a function of u. The numerical results are again in good agreement with the predictions of exponents and prefactors in Eq. (B14).

[1] V. V. Ivanov, Astron. Astrophys. **286**, 328 (1994).

[2] U. Frisch and H. Frisch, in *Lévy Flights and Applications,* edited by G. Zaslavsky, M. F. Shlesinger, and U. Frisch (Springer, Berlin, in press).

[3] Y. E. Koo, R. Kopelman, A. Yen, and A. Lin, in *Dynamics in Small Confining Systems,* edited by J. M. Drake, J. Klafter, R. Kopelman, and D. D. Awschalom, MRS Symposia Proceedings No. 290 (Materials Research Society, Pittsburgh, 1993), p. 273.

[4] E. W. Montroll and B. J. West, in *Fluctuation Phenomena,* edited by E. W. Montroll and J. L. Lebowitz (North-Holland, Amsterdam, 1976), p. 61.

[5] H. S. Carlslaw and J. C. Jaeger, *Conduction of Heat in Solids* (Clarendon, Oxford, 1978).

[6] P. Henrici, *Applied and Computational Complex Analysis* (Wiley, New York, 1986).

[7] H. Primas (unpublished).

[8] S. Havlin, H. Larralde, R. Kopelman, and G. H. Weiss,

Physica A **169**, 337 (1990).
[9] H. Taitelbaum and G. H. Weiss, Phys. Rev. E **50**, 2357 (1994).
[10] J. Klafter, G. Zumofen, and A. Blumen, Chem. Phys. **177**, 821 (1993).
[11] G. Zumofen and J. Klafter, Phys. Rev. E **47**, 851 (1993).
[12] G. Zumofen and J. Klafter, Europhys. Lett. **26**, 565 (1994); J. Klafter and G. Zumofen, Phys. Rev. E **49**, 4873 (1994).
[13] M. F. Shlesinger and J. Klafter, Phys. Rev. Lett. **54**, 2551 (1985).
[14] G. Zumofen and J. Klafter, Chem. Phys. Lett. **219**, 303 (1994).
[15] M. F. Shlesinger, G. Zaslavsky, and J. Klafter, Nature **263**, 31 (1993).
[16] G. Trefán, E. Floriani, B. J. West, and P. Grigolini, Phys. Rev. E **50**, 2564 (1994).
[17] W. Feller, *An Introduction to Probability Theory and its Applications* (Wiley, New York, 1971), Vol. 2.
[18] E. W. Montroll and G. H. Weiss, J. Math. Phys. **6**, 167 (1965).
[19] G. Zumofen and J. Klafter (unpublished).
[20] G. Zumofen and J. Klafter, Phys. Rev. E **50**, 5119 (1994).
[21] *Handbook of Mathematical Functions,* edited by M. Abramowitz and I. A. Stegun (Dover, New York, 1972).